

E. LEVEUGLE
L.V. ZHIGILEI✉

Microscopic mechanisms of short pulse laser spallation of molecular solids

Department of Materials Science & Engineering, University of Virginia, 116 Engineer's Way, Charlottesville, Virginia 22904-4745, USA

Received: 1 October 2003/Accepted: 22 January 2004
Published online: 26 July 2004 • © Springer-Verlag 2004

ABSTRACT The mechanisms of photomechanical spallation are investigated in a large-scale MD simulation of laser interaction with a molecular target performed in an irradiation regime of inertial stress confinement. The relaxation of laser-induced thermoelastic stresses is found to be responsible for the nucleation, growth, and coalescence of voids in a broad sub-surface region of the irradiated target. The depth of the region subjected to void evolution is defined by the competition between the evolving tensile stresses and thermal softening of the material due to the laser heating. The initial void volume distribution obtained in the simulation of laser spallation can be well described by a power law. A similar volume distribution is obtained in a series of simulations of uniaxial expansion of the same molecular system performed at a strain rate and temperature realized in the irradiated target. Spatial and time evolution of the laser-induced pressure predicted in the MD simulation of laser spallation is related to the results of an integration of a thermoelastic wave equation. The scope of applicability of the continuum calculations is discussed.

PACS 79.20.Ds; 61.80.Az; 02.70.Ns; 83.60.Uv

1 Introduction

The effect of laser irradiation on a target material is commonly discussed in terms of laser melting, evaporation from the irradiated surface, and, at higher laser fluences, overheating and explosive boiling of a surface region of the target. There is growing experimental evidence, however, that photomechanical processes related to the relaxation of laser-induced stresses can play a significant role in defining the outcome of short-pulse laser irradiation [1–5]. Examples of phenomena typically attributed to photomechanical processes include energetically efficient laser ablation by mechanical disintegration/spallation and ejection of chunks of solid material, sub-surface cavitation and expulsion of large droplets from a liquid/melted target [1, 3, 4], and low-energy laser damage of biological tissues [5] and systems with spatially-localized absorbing structures [6, 7].

The majority of theoretical and computational investigations of photomechanical effects are based on solving

a thermoelastic wave equation and predicting the evolution of stresses in the irradiated target [1, 3, 4, 7–9]. Surface displacements predicted in the simulations have been related to experimental measurements [8], whereas the evolution of tensile stresses in the target have been used to explain, at a qualitative level, the effects of cavitation and spallation of the target [1, 3, 4, 7]. The onset of void nucleation breaks the assumption of thermoelastic material response to laser heating. More complex hydrodynamic computational models have been used to describe the evolution of photomechanical damage under the action of laser-induced tensile stresses [10, 11]. Hydrodynamic codes capable of simulation of laser damage and spallation have to include a number of assumptions on the kinetics of void nucleation and evolution under the action of laser-induced stresses and the initial density/distribution of void nucleation sites, as well as the effect of temperature and deformation rate on the processes of void nucleation and growth.

An alternative method of microscopic analysis of laser-induced processes is the molecular dynamics (MD) computer simulation technique. The advantage of MD is that the only input in the model is the description of interatomic/intermolecular interaction, and no assumptions are made about the processes to be investigated. In this work we use the results of a large-scale MD simulation of laser interaction with a molecular solid to perform a detailed microscopic analysis of void nucleation, growth, and coalescence in photomechanical spallation. The results of the MD simulation are related to the prediction of a continuum model for the evolution of thermoelastic stresses. The physical mechanisms of laser spallation are also discussed.

2 Computational method

Laser interaction with an amorphous molecular target is simulated with the ‘breathing sphere’ model [12] that adapts a coarse-grained representation of molecules by particles with real translational degrees of freedom, but approximate representation of the internal degrees of freedom. The model provides an adequate description of molecular excitation by laser irradiation, intermolecular energy transfer, as well as the collective molecular dynamics induced by laser irradiation [12, 13]. A large computational cell with dimensions of $40 \times 40 \times 90$ nm (1 015 072 molecules) is used in the simulation to ensure that the periodic boundary condi-

✉ Fax: +1-434/982-5660, E-mail: lz2n@virginia.edu

tions imposed in the directions parallel to the surface do not affect the early evolution of the photomechanical damage investigated in this paper. The values of the laser pulse duration of 15 ps and an absorption depth of 50 nm are chosen so that the condition of stress confinement is satisfied [14]. Laser fluence of 31 J/cm² is chosen to be close to the threshold for laser spallation as determined in earlier smaller-scale simulations [14, 15].

To compare the predictions of MD simulations with a simple thermoelastic material response to the fast laser heating we perform a numerical integration of a one-dimensional wave equation,

$$\frac{1}{c^2} \frac{\partial^2 u}{\partial t^2} = \frac{\partial^2 u}{\partial x^2} - \alpha \frac{\partial \theta}{\partial x}$$

where u is the longitudinal displacement, α is the volume coefficient of thermal expansion, $\theta = T - T_0 = \Delta E/C_v$ is the temperature rise due to the laser energy deposition, T_0 is the initial temperature of the target, and C_v is the heat capacity. Neglecting heat conduction and assuming Lambert–Beer's law and a Gaussian temporal profile we can describe the laser energy deposition as:

$$\Delta E = I_0(1 - R)L_p^{-1} \exp\left(-\frac{x}{L_p}\right) \frac{1}{\sigma\sqrt{2\pi}} \int_0^t \exp\left(-\frac{(t-t_0)^2}{2\sigma^2}\right) dt,$$

where I_0 is the peak intensity, R is the reflectivity, L_p is the optical absorption depth, and σ is the standard deviation of the Gaussian profile, related to the pulse duration as $\tau_L = FWHM = \sigma\sqrt{8\ln(2)}$. Laser fluence F is related to the peak intensity I_0 as $F = \sqrt{\pi/4\ln(2)}\tau_L I_0 \approx 1.0645\tau_L I_0$. The absorbed laser fluence, related to the incident fluence as $F_{\text{abs}} = F(1 - R)$, is used in the discussion of the simulation results in this paper. Thermoelastic stresses can be calculated from the displacements, $\sigma_{xx} = c^2 \varrho (\partial u / \partial x - \alpha \theta)$, where σ_{xx} is the normal stress, and ϱ the density. Materials parameters in the continuum calculations are chosen to match the ones determined for the model molecular solid represented by the breathing sphere model, so that quantitative comparison between the results of the MD simulation and numerical solutions of the wave equation can be made. In order to account for the time of the energy transfer from the internal energy of excited molecules to the thermal energy of translational molecular motion, the laser pulse duration in the continuum simulations is taken to be longer as compared to the MD simulation.

3 Results and discussion

The spatial distributions of temperature, pressure, and void fraction are shown in Fig. 1 for four different times following the laser irradiation. The temperature profiles are largely defined by laser energy deposition, which follows the Lambert–Beer law and leads to an exponential decrease of the energy density with depth. Noticeable deviations of the temperature profiles from the exponential decay can be related to the evolution of pressure in the surface region of the target. The initial energy deposition, occurring under conditions of inertial stress confinement [1, 14], leads to the build

up of high compressive thermoelastic pressure. The interaction of the initial compressive pressure with the free surface of the target results in the development of a tensile component of the thermoelastic pressure wave that propagates into the bulk of the target. Comparison of the temperature and pressure profiles suggests that a transient cooling of the material (shoulders in the temperature profiles shown for 30 and 50 ps) correlates with the development of the tensile component of the pressure wave. Considering a fast adiabatic/isentropic expansion of a material, the temperature variation with pressure can be estimated from classical thermodynamics, $(\partial T / \partial P)_s = VT\alpha / C_p > 0$, where the heat capacity C_p , volume V , and the volume coefficient of thermal expansion α are all positive for the model molecular material. Similar temperature–pressure correlations have been recently observed and discussed for simulations of laser interaction with metal films [16] and bulk targets [17]. Additional factors affecting the temperature evolution are the nucleation and growth of voids, as well as evaporation from the surface, both leading to temperature decrease. Thermal conduction to the bulk of the molecular target is slow and has a negligible effect on the temperature profile over the timescale of the simulation.

Pressure profiles observed in the MD simulation, Fig. 1, agree relatively well with the results of numerical integration of the wave equation, Fig. 2a. The tensile component of the pressure wave increases with time and depth, and reaches the maximum values of -170 MPa at 50 ps, -180 MPa at 70 ps, and -240 MPa at 90 ps. A slower, as compared to the prediction of the wave equation, increase of the maximum tensile stresses between 50 ps and 70 ps can be attributed to void nucleation. The tensile stresses cannot exceed the dynamic strength of the material, which is a function of temperature and increases with depth.

The appearance and growth of voids in the surface region of the irradiated target are visualized in snapshots shown in the left frames of Fig. 1. In these snapshots each void is represented by an individual sphere of the same volume as the actual void. The voids are defined by superimposing molecular configuration with a three-dimensional grid of cubic cells with a size of 0.68 nm and identifying cells that do not contain any molecules. Voids are defined as clusters of more than 2 empty cells connected with each other by sharing a face. The appearance of a large number of small voids at 30 ps and 50 ps can be correlated with the appearance and propagation of the tensile component of the pressure wave. Although larger tensile stresses are created as the pressure wave propagates deeper into the sample, they do not lead to void nucleation in a colder and stronger material. All the photomechanical damage is localized within ~ 40 nm surface region.

The initial volume distribution of voids that appear around the time of 30 ps can be well described by a steep power law, $N(V) = N_0 \times V^{-\tau}$, with an exponent $-\tau = -3.38$, Fig. 3. Additional smaller points shown in Fig. 3 correspond to the volume distribution of voids generated in eight smaller scale MD simulations of a homogeneous uniaxial expansion of a molecular system. The temperature and the strain rate used in these simulations correspond to the conditions realized at a depth of 10 nm in an irradiated molecular target. The strain rate is obtained from the solution of the wave equation. As shown in Fig. 2b, the strain evolution with time predicted by

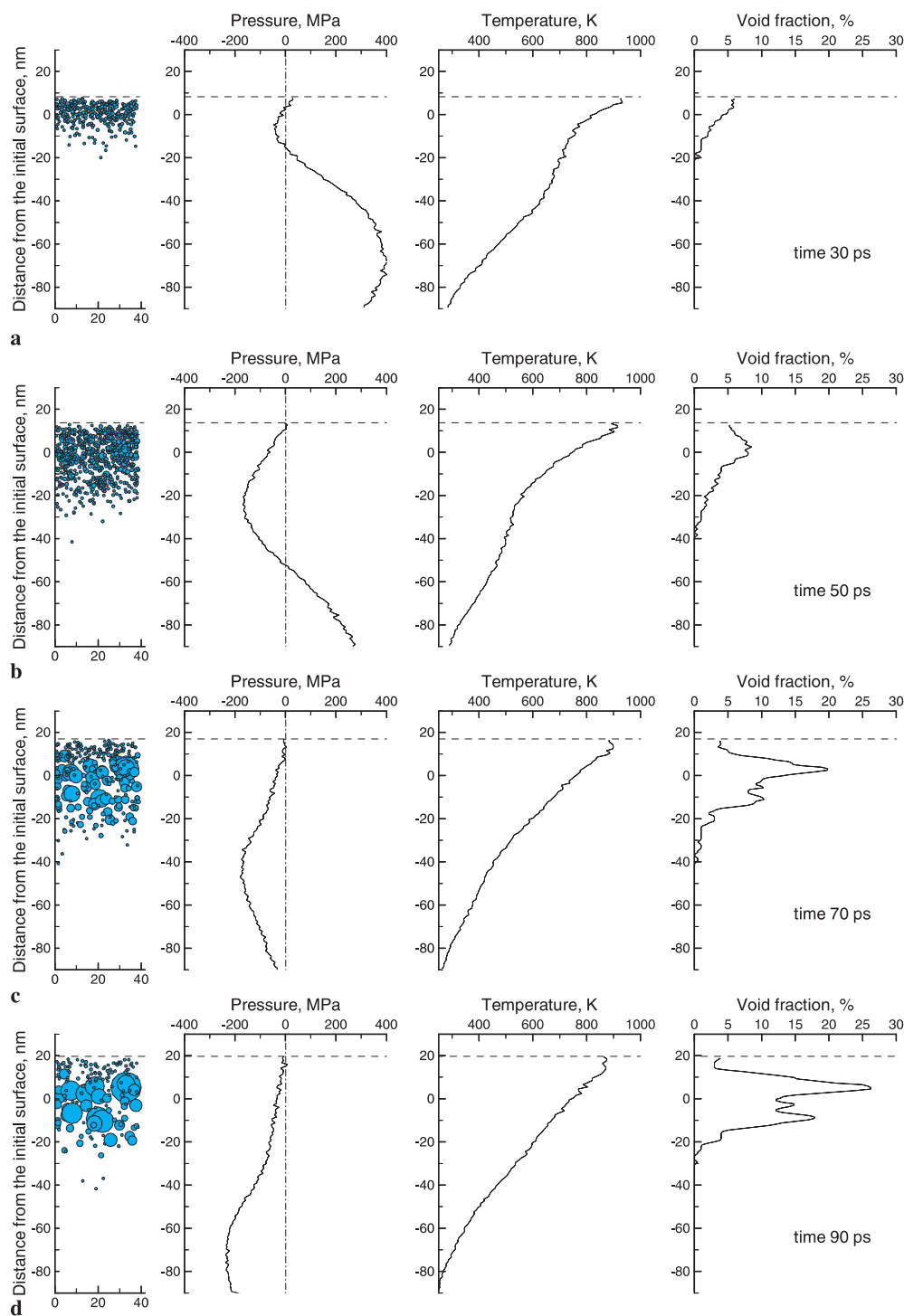


FIGURE 1 Distribution of voids, pressure, temperature, and volume fraction of voids in a molecular target irradiated with a 15 ps laser pulse at a fluence of 31 J/m^2 shown for 30 ps (a), 50 ps (b), 70 ps (c), and 90 ps (d) after the beginning of the laser pulse. In the left frames the voids are represented by spheres of the same volume as the actual voids. Horizontal dashed lines show current locations of the surface

the wave equation and observed in the large-scale MD simulation of laser interaction with a molecular target are almost identical up to the time of ~ 30 ps. At later times, after the onset of void nucleation, the assumption of thermoelastic material response to laser heating is no longer valid and the strain evolution observed in the MD simulation is affected by void nucleation and growth.

An agreement between the volume distributions of voids observed in the MD simulation of laser irradiation and the small-scale MD simulations of uniaxial expansion of the same

molecular system is surprisingly good, taking into account that the simulations of uniaxial expansion reproduce the conditions realized at a specific depth under the surface, whereas the results for laser induced void nucleation include contributions from the whole surface region. This good agreement may be indicative of a general characteristic of void nucleation at high strain rates and elevated temperatures. Indeed, a power law mass distribution has been predicted for fragmentation resulting from the interaction of a shock wave with a surface [18], as well as for the cluster size distributions ob-

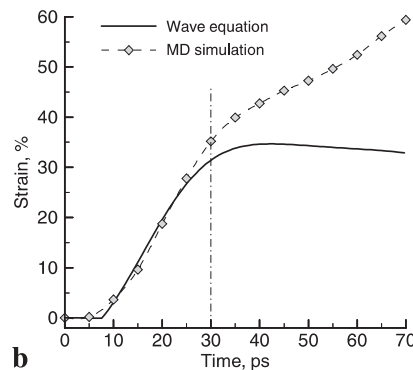
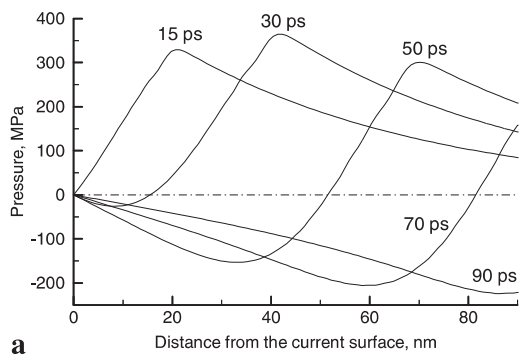


FIGURE 2 Thermoelastic pressure wave (a) and strain evolution at a depth of 10 nm under the surface (b) predicted by the wave equation for irradiation conditions used in the MD simulation illustrated in Fig. 1. Strain evolution obtained in the MD simulation is also shown in b by solid diamonds connected by a dashed line

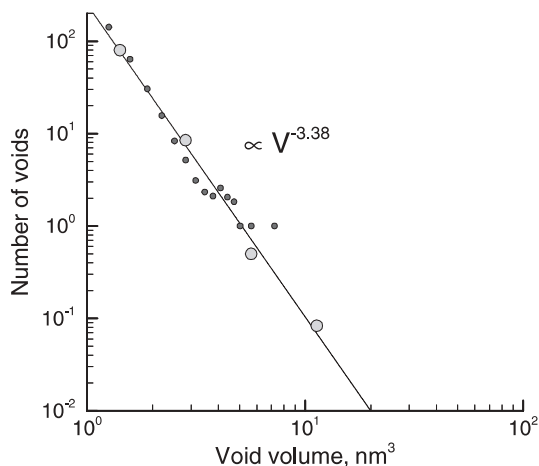


FIGURE 3 Void size distribution obtained in an MD simulation of laser spallation of a molecular target irradiated by a 15 ps laser pulse at a fluence of 31 J/m^2 (large dots) and in a series of eight MD simulations of uniaxial expansion of a molecular solid performed for the conditions realized at a depth of 10 nm of the irradiated molecular system (small dots). The line is a power law fit of the data points with the exponent indicated in the figure

served in a recent computational study of laser ablation [19]. A power law void volume distribution has been also reported in an MD simulation of back spallation in a metal film subjected to a high velocity impact [20].

The evolution of voids in the simulation illustrated by Fig. 1 can be separated into two stages. At the initial stage of void nucleation and growth the number of voids of all sizes increases with time. At the second stage of void coarsening and coalescence, starting from ~ 50 ps, the number of large voids increases while the number of small voids decreases. With the omission of the smallest voids, the void volume distributions at longer times can be still relatively well described by the power law with an exponent increasing with time (the absolute value of $-\tau$ decreases) [17]. By the time of 90 ps a few very large voids account for the majority of empty volume in the subsurface region of the target. Further growth and coalescence of the large voids lead to the separation and ejection of large clusters.

The results of a large-scale MD simulation of short pulse laser interaction with a molecular target provide a detailed microscopic picture of the mechanisms of laser spallation. The relaxation of laser-induced thermoelastic stresses results in the nucleation, growth and coalescence of voids in a broad

surface region of the irradiated target. The mechanical stability of the target material is strongly affected by laser heating, and the depth of the region subjected to void evolution is defined by competition between the tensile stresses that are increasing with depth and the decreasing thermal softening. Observation of void generation and evolution in a broad subsurface region of irradiated target agrees with experimental observations of laser-induced cavitation in aqueous solutions and biological tissues [1, 4, 21]. Preliminary results of the simulations of laser spallation of metal targets [16, 17] suggest that the mechanisms of photomechanical damage and spallation discussed above for molecular systems may be operational in other material systems as well.

ACKNOWLEDGEMENTS Partial financial support of this work was provided by the Air Force Office of Scientific Research through the Medical Free Electron Laser Program.

REFERENCES

- 1 G. Paltauf, P.E. Dyer: Chem. Rev. **103**, 487 (2003)
- 2 R. Cramer, R.F. Haglund Jr., F. Hillenkamp: Int. J. Mass Spectrom. Ion Processes **169/170**, 51 (1997)
- 3 R.L. Webb, J.T. Dickinson, G.J. Exarhos: Appl. Spectrosc. **51**, 707 (1997)
- 4 D. Kim, M. Ye, C.P. Grigoropoulos: Appl. Phys. A **67**, 169 (1998)
- 5 A. Vogel, V. Venugopalan: Chem. Rev. **103**, 321 (2003)
- 6 S.L. Jacques, A.A. Oraevsky, R. Thompson, B.S. Gerstman: Proc. SPIE **2134A**, 54 (1994)
- 7 G. Paltauf, H. Schmidt-Kloiber: Appl. Phys. A **68**, 525 (1999)
- 8 I. Itzkan, D. Albagli, M.L. Dark, L.T. Perelman, C. Von Rosenberg, M.S. Feld: Proc. Natl. Acad. Sci. USA **92**, 1960 (1995)
- 9 X. Wang, X. Xu: Appl. Phys. A **73**, 107 (2001)
- 10 T. Antoun, L. Seaman, M.E. Glinsky: SPIE **2391**, 413 (1995)
- 11 M. Strauss, Y. Kaufman, M. Sapir, P.A. Amendt, R.A. London, M.E. Glinsky: J. Appl. Phys. **91**, 4720 (2002)
- 12 L.V. Zhigilei, E. Leveugle, B.J. Garrison, Y.G. Yingling, M.I. Zeifman: Chem. Rev. **103**, 321 (2003)
- 13 L.V. Zhigilei, Y.G. Yingling, T.E. Itina, T.A. Schoolcraft, B.J. Garrison: Int. J. Mass Spectrom. **226**, 85 (2003)
- 14 L.V. Zhigilei, B.J. Garrison: J. Appl. Phys. **88**, 1281 (2000)
- 15 A.G. Zhidkov, L.V. Zhigilei, A. Sasaki, T. Tajima: Appl. Phys. A **73**, 741 (2001)
- 16 D.S. Ivanov, L.V. Zhigilei: Phys. Rev. B **68**, 064 114 (2003); *ibid.*, Phys. Rev. Lett. **91**, 105 701 (2003)
- 17 E. Leveugle, D.S. Ivanov, L.V. Zhigilei: Appl. Phys. A, in press
- 18 I.S. Bitensky, E.S. Parilis: Nucl. Instrum. Methods Phys. Res. B **21**, 26 (1987)
- 19 L.V. Zhigilei: Appl. Phys. A **76**, 339 (2003)
- 20 A. Strachan, T. Çağın, W.A. Goddard III: Phys. Rev. B **63**, 060 103 (2001)
- 21 A.A. Oraevsky, R. Esenaliev, S.L. Jacques, F.K. Tittel: SPIE Proc. Series **2391**, 300 (1995)